European Journal of Taxonomy 1048: 202–222
https://doi.org/10.5852/ejt.2026.1048.3247
europeanjournaloftaxonomy.eu
ISSN 2118-9773
2026 · Wang B. *et al.*

Received: 26 September 2025 • *Accepted: 11 February 2026* • *Published: 9 April 2026*

Topic editor: Magalie Castelin • *Desk editor: Pepe Fernández*

Research article

urn:lsid:zoobank.org:pub:DB9809A8-CF0C-4E45-8CDA-F6EA6183C894

Integrative taxonomy reveals a new cryptic species of *Raphidopus* Stimpson, 1858 (Decapoda, Anomura, Porcellanidae) from the Yellow Sea and East China Sea

Bin WANG [1], Yuhan WAN [2], Xuefeng FANG [3], Jian-Wen QIU [4] & Dong DONG [5,*]

[1,2,5] Laboratory of Marine Organism Taxonomy and Phylogeny, Shandong Province Key Laboratory of Marine Biodiversity and Bio-resource Sustainable Utilization, Institute of Oceanology, Chinese Academy of Sciences, Qingdao 266071, China.
[1,2,5] College of Marine Science, University of Chinese Academy of Sciences, Beijing, China.
[3] State Environmental Protection Key Laboratory of Coastal Ecosystem, National Marine Environmental Monitoring Center, Dalian, China.
[4] Southern Marine Science and Engineering Guangdong Laboratory (Guangzhou), Guangzhou 511458, China.
[4] Department of Biology, Hong Kong Baptist University, Hong Kong SAR, China.

[*] Corresponding author: dongd@qdio.ac.cn
[1] Email: wangbin@qdio.ac.cn
[2] Email: wanyuhan@qdio.ac.cn
[3] Email: xffang@nmemc.org.cn
[4] Email: qiujw@hkbu.edu.hk

Abstract. *Raphidopus ciliatus* Stimpson, 1858 is believed to be widely distributed across the Indo-West Pacific and has been reported along the entire coast of China. However, molecular and morphological analyses reveal the presence of a cryptic species in northern Chinese waters, described herein as *R. xinzhengi* Dong, Wan & Wang sp. nov. The COI sequences of the two species of *Raphidopus* show 8.7–9.0% divergence, higher than each intraspecific variation. The new species can be distinguished from *R. ciliatus* primarily by the arrangement of granules on the cheliped carpus, the length/width ratio of the cheliped carpus, and the length/width ratio of the merus of the first ambulatory leg. An updated key to the species of the genus *Raphidopus* is provided.

Keywords. China seas, phylogeny, porcelain crab, taxonomy, West Pacific.

Wang B., Wan Y., Fang X., Qiu J.-W. & Dong D. 2026. Integrative taxonomy reveals a new cryptic species of *Raphidopus* Stimpson, 1858 (Decapoda, Anomura, Porcellanidae) from the Yellow Sea and East China Sea. *European Journal of Taxonomy* 1048: 202–222. https://doi.org/10.5852/ejt.2026.1048.3247

Introduction

Raphidopus Stimpson, 1858 is a genus of porcelain crabs that typically inhabit muddy bottoms of shallow waters; some species are reported as commensal with polychaetes (Osawa & Ng 2018). Members of the genus are widely distributed across the Indo-West Pacific, from the Persian Gulf to Japan and Australian waters (Grant & McCulloch 1906; Miyake 1943; Haig 1966; Ng *et al.* 2012; Osawa & Ng 2018). The genus currently comprises six valid species: *R. ciliatus* Stimpson, 1858, *R. indicus* Henderson, 1893, *R. johnsoni* Ng & Nakasone, 1994, *R. persicus* Ng, Safaie & Naser, 2012, *R. brevipes* Osawa & Ng, 2018, and *R. dhritiae* Mitra, Chowdhury & Bose, 2025. Three of these species have been recorded in the West Pacific: *R. ciliatus*, *R. johnsoni* and *R. brevipes*, and the former two species are restricted to Peninsular Malaysia and Java Island (Osawa & Ng 2018), while *R. ciliatus* is recorded across the western Pacific from north China to southeast Australia and the Arabian Sea (Grant & McCulloch 1906; Miyake 1943; Haig 1965, 1992; Tirmizi & Ghani 1994). In the Chinese seas, *R. ciliatus* has been reported along the entire coastline, and specimens from different localities have traditionally been treated as conspecific. However, material from northern China, including the Yellow Sea and East China Sea, exhibits several morphological and coloration differences from that of the type locality Hong Kong, China, and other populations in the South China Sea. In this study, we employ an integrative approach, combining molecular data and morphological comparisons to assess the taxonomic status of populations from the northern and southern China seas. We reveal a previously unrecognized species from north Chinese waters. The new species and *R. ciliatus* are described and illustrated in detail herein.

Material and methods

Sample collection and morphological examination

Specimens were collected from 11 locations along the Chinese coastline (Fig. 1). All specimens examined were fixed in 95% ethanol and deposited in the Marine Biodiversity Museum (MBM), Chinese Academy of Sciences. Morphological examinations and descriptive terminology mainly follow Osawa & Ng (2018). Size of the specimens examined is shown as carapace length (CL), measured from the tip of the median rostral lobe to the median point of the posterior margin of the carapace.

DNA sequening and phylogenetic analyses

Genomic DNA was extracted from abdominal muscle tissue using the TIANGEN Marine Animal DNA Kit (TIANGEN, Beijing, China). A fragment (657-bp) of the cytochrome c oxidase subunit I (COI) gene was amplified by polymerase chain reaction (PCR) with primers HCO2198 and LCOgala (Folmer *et al.* 1994; Dong *et al.* 2019) following the original protocol. PCR products were then commercially purified and sequenced by Tsingke Biotechnology Co., Ltd. (Qingdao, China). Contigs were assembled and verified from bidirectional sequences using the SeqMAN module in DNASTAR ver. 7.1 (Burland 2000). *Pisidia serratifrons* (Stimpson, 1858) was used as outgroup (Table 1).

The sequences were aligned using MEGA ver. 7.0 (Kumar *et al.* 2016) and then manually trimmed. The inter- and intraspecific genetic distances of species of *Raphidopus* were obtained using the Kimura two-parameter model (K2P; Kimura 1980) in MEGA ver. 7.0 using COI sequences. Phylogenetic analyses were conducted using Bayesian (BI) and maximum likelihood (ML) methods. The best-fit substitution model (HKY+I+F) was identified using ModelFinder (Kalyaanamoorthy *et al.* 2017) based on the Bayesian Information Criterion (Schwarz 1978). Bayesian Inference phylogenies were inferred using MrBayes ver. 3.2.6 (Ronquist *et al.* 2012) with 1 000 000 generations and the initial 25% of sampled data was discarded as burn-in; the nodal support was assessed with posterior probabilities (PP). Maximum likelihood phylogenies were inferred using IQ-TREE (Nguyen *et al.* 2015) for 1000 standard bootstrap replicates to estimate the bootstrap support (BS) value on each node. All the analyses mentioned above were performed using the integrated and scalable desktop platform PhyloSuites ver. 1.2.2 (Zhang *et al.*

2020). The phylogenetic trees were visualized using the iTOL webserver (Letunic & Bork 2021). Species boundaries were initially delineated based on interlineage genetic distances. Haplotype information was obtained using DnaSP ver. 6 (Rozas *et al.* 2017). The haplotype network of genetic connections between geographic groups and species was generated with the TCS method in PopART ver. 1.7 (Leigh & Bryant 2015).

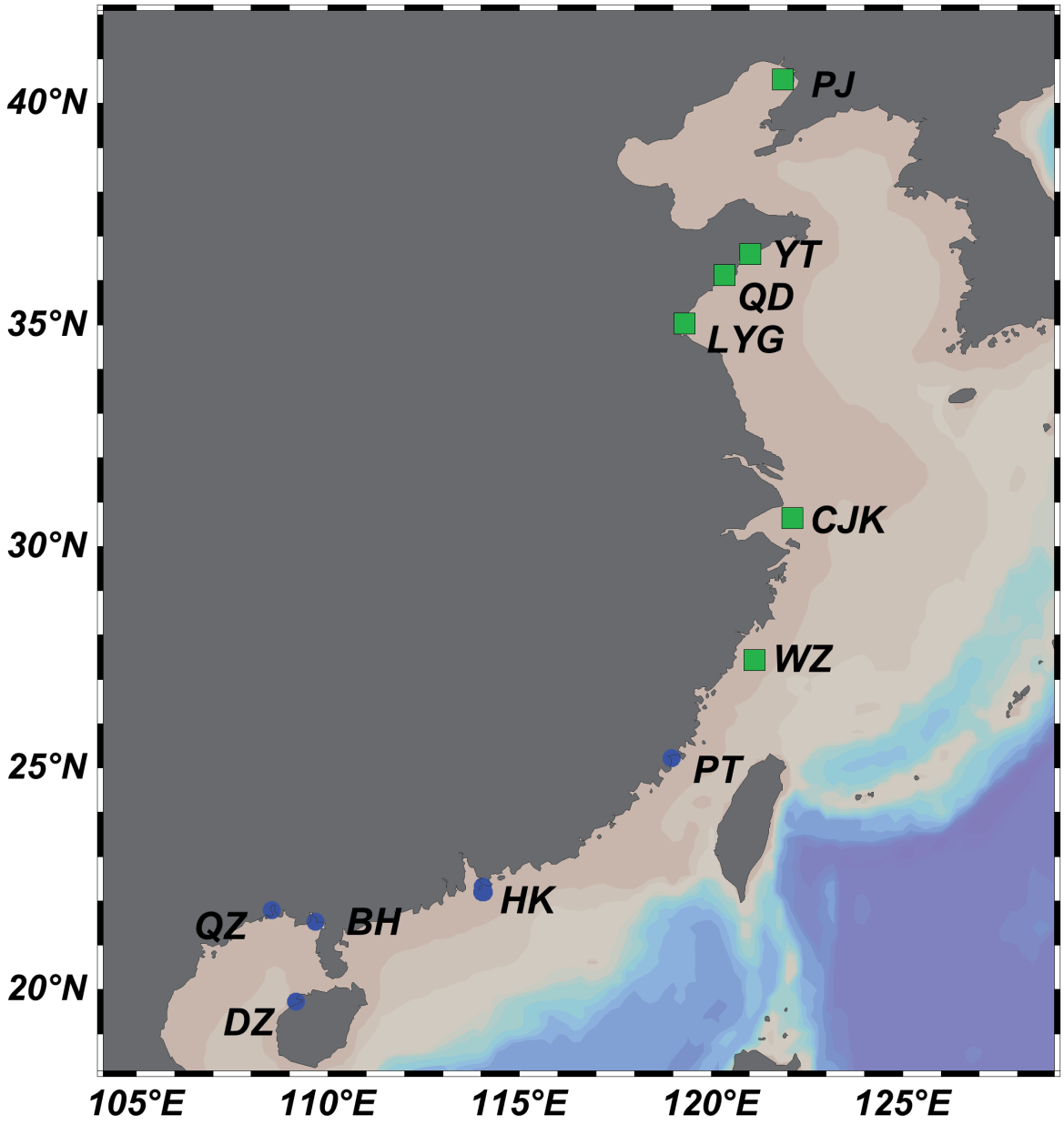

Fig. 1. Sampling localities of the two species in this study. Green squares denote collection localities for *Raphidopus xinzhengi* Dong, Wan & Wang sp. nov. and the blue circles represent those for *R. ciliatus* Stimpson, 1858. Locality abbreviations: BH = Beihai; CJK = Yangtze River Estuary; DZ = Danzhou; HK = Hong Kong; LYG = Lianyungang; PJ = Panjin; PT = Putian; QD = Qingdao; QZ = Qinzhou; YT = Yantai; WZ = Wenzhou.

Table 1. List of species and specimens incorporated in the phylogenetic analysis, along with corresponding collection localities, COI gene haplotypes, GenBank accession numbers and references. Each specimen represents a population from a distinct locality. All the four haplotypes recovered from the TCS network were included in the phylogenetic analysis. The four GenBank accession numbers generated in this study correspond to the four identified haplotypes. *Pisidia serratifrons* (Stimpson, 1858) is the outgroup.

Species/specimens	Localities	Haplotype	GenBank accession number	Reference
Raphidopus xinzhengi Dong, Wan & Wang sp. nov.				
QD-Holotype	Qingdao, China	Hap-3	PX405584	This study
YT-Paratype	Yantai, China	Hap-1	PX405585	This study
PJ	Panjin, China	Hap-2	PX405586	This study
WZ	Wenzhou, China	Hap-3	–	This study
CJK	Yangtze River Estuary, China	Hap-1	–	This study
Raphidopus ciliatus Stimpson, 1858				
HK-C1	Hong Kong, China	Hap-4	PX405587	This study
HK-C2	Hong Kong, China	Hap-4	–	This study
HK-C3	Hong Kong, China	Hap-4	–	This study
PT	Putian, China	Hap-4	–	This study
DZ	Danzhou, China	Hap-4	–	This study
QZ	Qinzhou, China	Hap-4	–	This study
BH	Beihai, China	Hap-4	–	This study
Pisidia serratifrons (Stimpson, 1858)	–	–	OR460835	Fang *et al.* 2023

Results

Phylogenetics

642-bp segments of the COI gene from 34 specimens of *R. xinzhengi* Dong, Wan & Wang sp. nov. and *R. ciliatus* were generated in the present study. The average genetic distance (K2P) between *R. xinzhengi* and *R. ciliatus*, averaged at 8.7–9.0%. The intraspecific genetic distance for *R. xinzhengi* ranged from 0% to 0.4%, while that for *R. ciliatus* ranged from 0% to 0.1%. The phylogenetic trees constructed based on Maximum Likelihood (ML) analysis and Bayesian Inference (BI) are entirely congruent, revealing two well-supported, distinct clades that represent the two species of *Raphidopus*. Within the phylogenetic tree, each species of *Raphidopus* forms a distinct, well-supported clade (Fig. 2). The presence of two distinct haplotype groups in the TCS network, corresponding to *R. xinzhengi* and *R. ciliatus*, is congruent with the phylogenetic trees, further supporting the delineation of these two species (Fig. 3). The network analysis reveals three haplotypes (Hap-1, Hap-2 and Hap-3) among the 19 individuals of *R. xinzhengi*. In contrast, all 15 individuals of *R. ciliatus* share a single haplotype (Hap-4), indicating a relatively low haplotype diversity in this species.

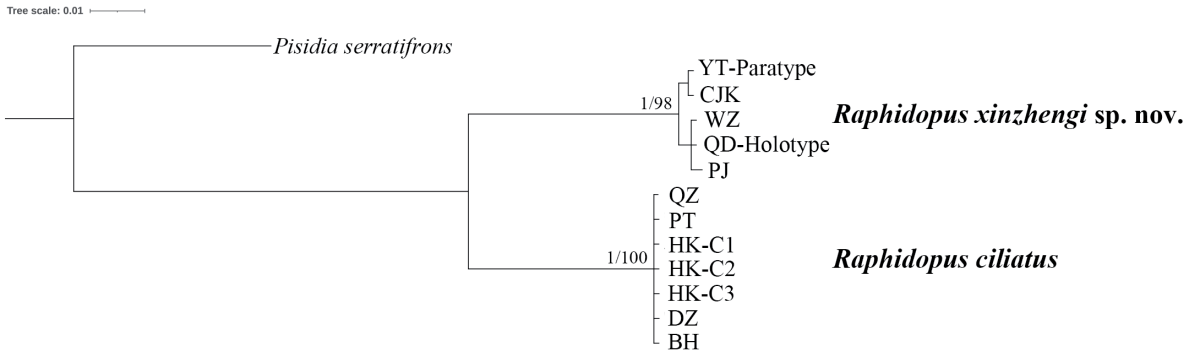

Fig. 2. Phylogenetic tree constructed based on the COI gene sequences of *Raphidopus xinzhengi* Dong, Wan & Wang sp. nov. and *R. ciliatus* Stimpson, 1858. Posterior probabilities (PP, left) and bootstrap support values (BS, right) are shown.

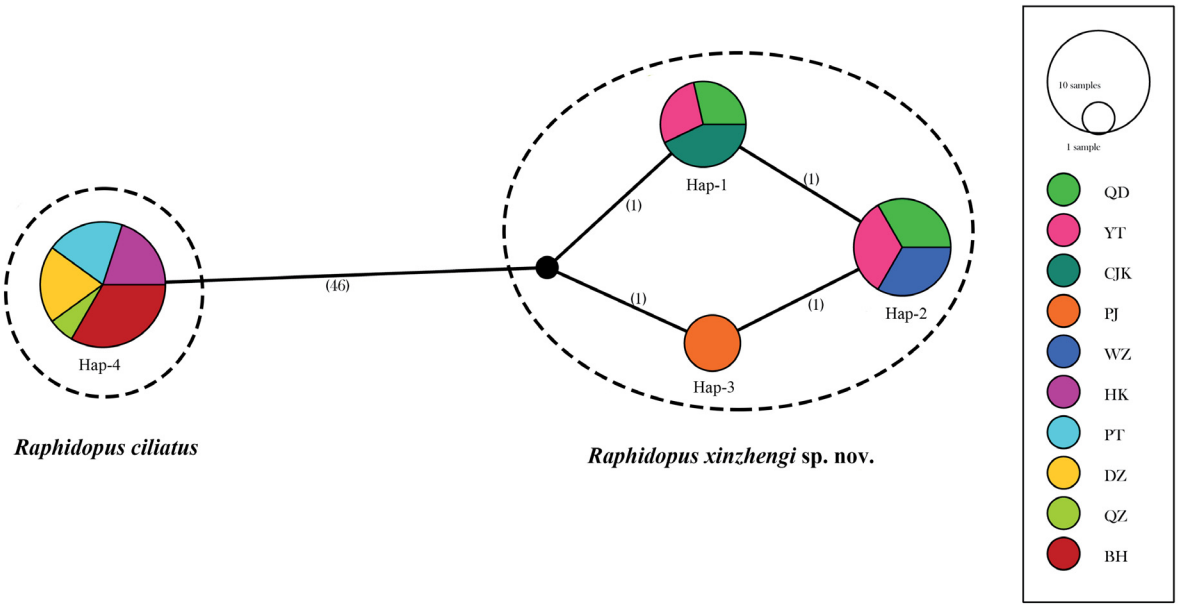

Fig. 3. Mitochondrial COI gene haplotype network for *Raphidopus ciliatus* Stimpson, 1858 and the new species *R. xinzhengi* Dong, Wan & Wang sp. nov. Each node denotes a unique haplotype, with area proportional to haplotype frequency (number of individuals). Geographic origins are indicated by color codes (see legend). Putative ancestral haplotypes or unsampled intermediates are represented by small black dots. Pie segments within nodes illustrate the regional distribution composition of each haplotype. Values along branches specify the number of mutational steps between haplotypes. Dashed ellipses of distinct colors denote different taxonomic groups.

Systematic account

Phylum Arthropoda von Siebold, 1848
Subphylum Crustacea Brünnich, 1772
Class Malacostraca Latreille, 1802
Order Decapoda Latreille, 1802
Infraorder Anomura MacLeay, 1838
Family Porcellanidae Haworth, 1825
Genus *Raphidopus* Stimpson, 1858

Raphidopus ciliatus Stimpson, 1858
Figs 1–3, 4A, 5–6

Raphidopus ciliatus Stimpson, 1858: 241 (type locality: Hong Kong, China).

Raphidopus ciliatus — Stimpson 1907: 185, pl. 22 fig. 5. — Henderson 1888: 113. — Grant & McCulloch 1906: 42. — Miyake 1943: 146, figs 61–62. — Haig 1965: 116; 1981: 274; 1992: 324, fig. 20. — Yang & Sun 1990: 12; 1992: 210, fig. 17; 2005: 26, fig. 22. — Ng & Nakasone 1994: 3, figs 1–2. — Tirmizi & Ghani 1994: 67, fig. 1 (part). — Hsieh *et al.* 1997: 351, figs 32g, 41. — Osawa & Chan 2010: 180, figs 141–142.

Diagnosis

Carapace broader than long, lateral margins with 2–4 distinct spines; hepatic margin separated from branchial margin by fissure or narrow V-shaped notch; dorsal surface with pair of oblique posterolateral ridges each armed with 1 or 2 strong median spine. Median lobe of thoracic sternite 3 comparatively high antero-posteriorly. Cheliped bearing long and thick plumose setae on margins and surfaces of all articles; carpus distinctly elongate, more than 2 times as long as broad, bearing bead-like granules regularly arranged on dorsoflexor margin; extensor margin with 4–7 strong spines; chela 2.5–3.0 times as long as broad, 1.3–1.8 times carapace width; palm with longitudinal groove on ventral surface near extensor margin. Ambulatory legs bearing long plumose setae; merus of second ambulatory leg 4.3–4.7 times as long as broad.

Material examined

CHINA – **northern South China Sea** • 1 ♂ (CL 10.2 mm); Hong Kong; 22°12′ N, 114°01′ E; 11 m depth; 11 May 2022; collected by bottom trawl; GenBank no.: PX405587; MBM287965 • 1 ♂ (CL 9.1 mm);

Fig. 4. Type specimens of two species of *Raphidopus* Stimpson, 1858 preserved in ethanol. **A**. *R. ciliatus* Stimpson, 1858, ♂, 10.2 mm (MBM287965), Hong Kong, China. **B**. *R. xinzhengi* Dong, Wan & Wang sp. nov., holotype, ♀, 8.3 mm (MBM287959), Jiaozhou Bay, Qingdao, China. Scale bars = 1.0 cm.

Hong Kong; 22°14′ N, 114°04′ E; 6 m depth; 13 Apr. 2022; collected by bottom trawl; MBM287966 • 3 ♂♂ (CL 6.5–8.0 mm); Hong Kong; 22°20′ N, 114°02′ E; 5 m depth; 28 Mar. 2023; collected by bottom trawl; MBM287967 • 4 ♂♂ (CL 7.5–8.5 mm); Guangxi Province, Shatian, Beihai; 21°32′ N, 109°40′ E; 6 m depth; 15 Oct. 2018; collected by bottom trawl; MBM287968 • 1 ♂ (CL 5.5 mm); Guangxi Province, Qinzhou; 21°48′ N, 108°32′ E; 10 m depth; 28 Mar. 2024; collected by bottom trawl; MBM287969 • 1 ♀ (CL 7.0 mm), 7 ♂♂ (CL 5.1–8.0 mm); Hainan Province, Danzhou; 19°44′ N, 109°10′ E; 9 m depth; 4 Jan. 2020; collected by bottom trawl; MBM287970. – **southern East China Sea** • 2 ♀♀ (CL 6.5–7.0 mm), 1 ♂ (CL 5.5 mm); Fujian Province, Putian; 25°14′ N, 118°58′ E; 10 m depth; 10 Nov. 2023; collected by bottom trawl; MBM287971.

Description

Carapace. 1.3 (1.2–1.4) times as broad as long, broadest at median branchial margin. Dorsal surface finely covered with numerous short striae, striae relatively long and elevated on lateral branchial and intestinal regions and usually bearing dense plumose setae; gastric and cardiac regions relatively glabrous, pair of protogastric ridges present; cervical grooves distinct. Hepatic margin convex, separated from branchial margin by fissure or narrow V-shaped notch. Branchial margins strongly convex, tuberculate, laterally expanded forming laminar ridges convergent posteriorly, armed with 2–4 distinct spines; oblique posterolateral ridge crenulate, extending onto posterior branchial region, bearing 1 or 2 strong median spine. Posterior margin straight. Rostrum short, trilobate; median lobe broad and bent ventrally, with short dorsomedian groove; lateral lobe approximately as broad as median lobe, slightly overreaching half of median lobe. Orbit concave; supra-ocular margins smooth; outer orbital angles bluntly triangular, reaching approximately half length of lateral rostral lobe. Pterygostomian flap entire; surface with longitudinal, long ridge on midline and several short, oblique rugae bearing thick plumose setae; anterior end produced, triangular.

Sternal plastron. Sternite 3 broad, trilobate; median lobe approximately 3.4 times as wide as high (width measured along anterior margin of sternite 3 excluding elongated lateral lobes), anterior margin straight or slightly convex; lateral lobes narrow, strongly produced anteriorly, reaching half of coxa of third maxilliped. Sternite 4 with anterior margin broadly concave, bearing submarginal row of thick plumose setae.

Telson. Composed of 7 plates.

Eye. Small, ocular peduncle short; distal margin of cornea slightly overreaching apex of lateral rostral lobe.

Basal article of antennular peduncle. Slightly longer than broad, with short transverse rugae on ventral surface; anterior margin weakly crenulated, mesial corner elevated and produced as rounded tooth.

Antennal peduncle. First article immovable, broad, anteriorly overreaching outer orbital corner; second to fourth articles (movable) subcylindrical, unarmed, third article longest.

Third maxilliped. Ischium rounded and lamellar, ventral surface with transverse rugae. Merus with rounded lobe on flexor margin, extensor margin straight; lateral surface with rugae. Carpus with rounded projection on median flexor margin. Propodus straight, elongate. Dactylus short. Rugae and margins of ischium and merus bearing dense plumose setae.

Cheliped. Unequal, bearing long and thick plumose setae on margins and surfaces of all articles, setae especially thicker on extensor and flexor margins of each article, ventral surface of merus and dorsal surface of chela. Merus robust, longer than broad, surfaces covered with numerous short rugae; dorsoflexor lobe low, marginally granulate, distally rounded, reaching or slightly overreaching distal

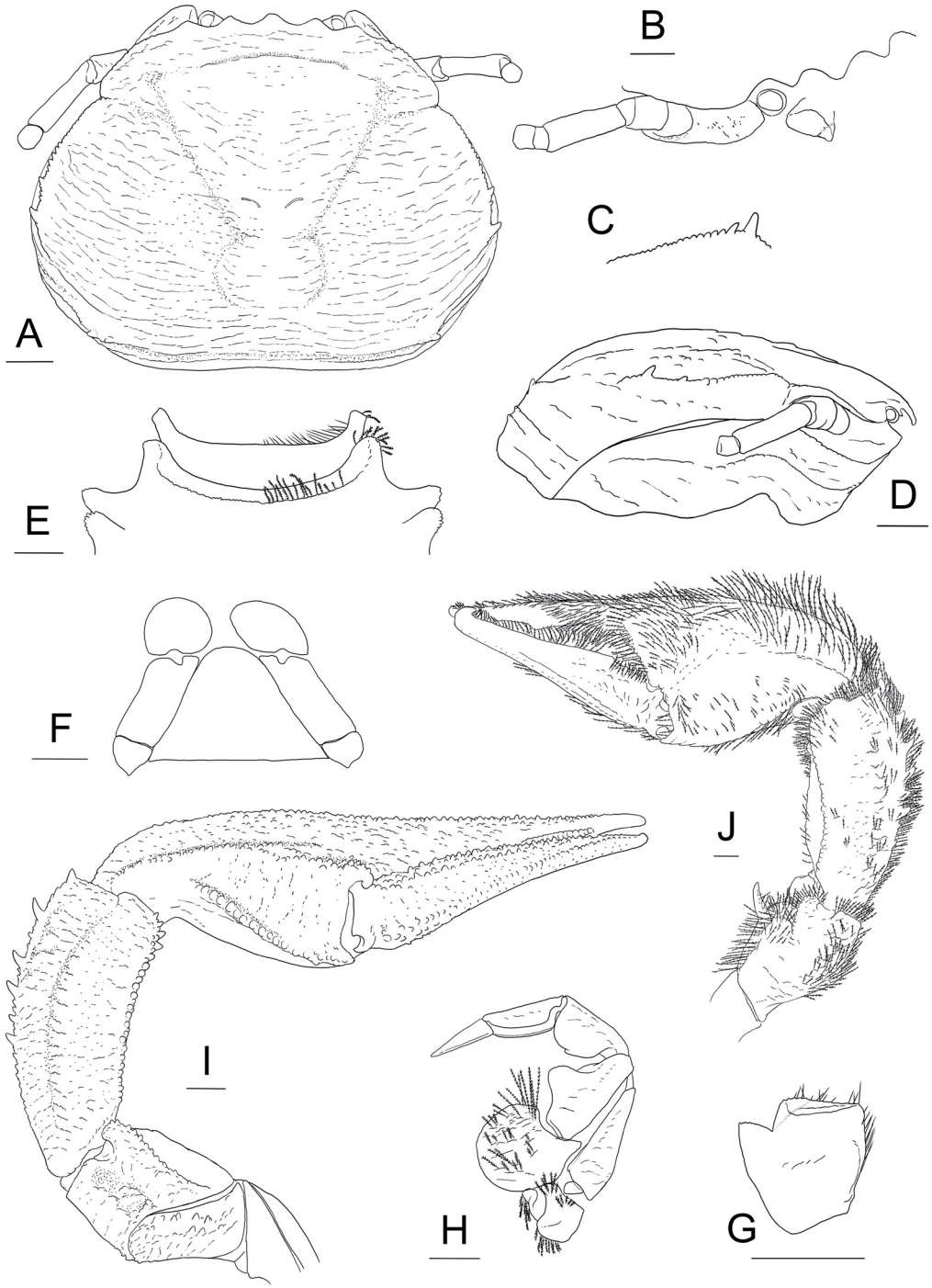

Fig. 5. *Raphidopus ciliatus* Stimpson, 1858, ♂, 10.2 mm (MBM287965), Hong Kong, China. **A**. Carapace, dorsal view. **B**. Right antennal peduncles and basal article of antennular peduncle, dorsolateral view. **C**. Posterolateral ridge of carapace. **D**. Right carapace and pterygostomian, lateral view. **E**. Third and fourth thoracic sternites (setae partially shown), ventral view. **F**. Telson, external view. **G**. Basal article of left antennular peduncle, ventral view. **H**. Left third maxilliped (setae partially shown), lateral view. **I**. Larger cheliped, dorsal view. **J**. Smaller cheliped (with setae), dorsal view. Scale bars = 1.0 mm.

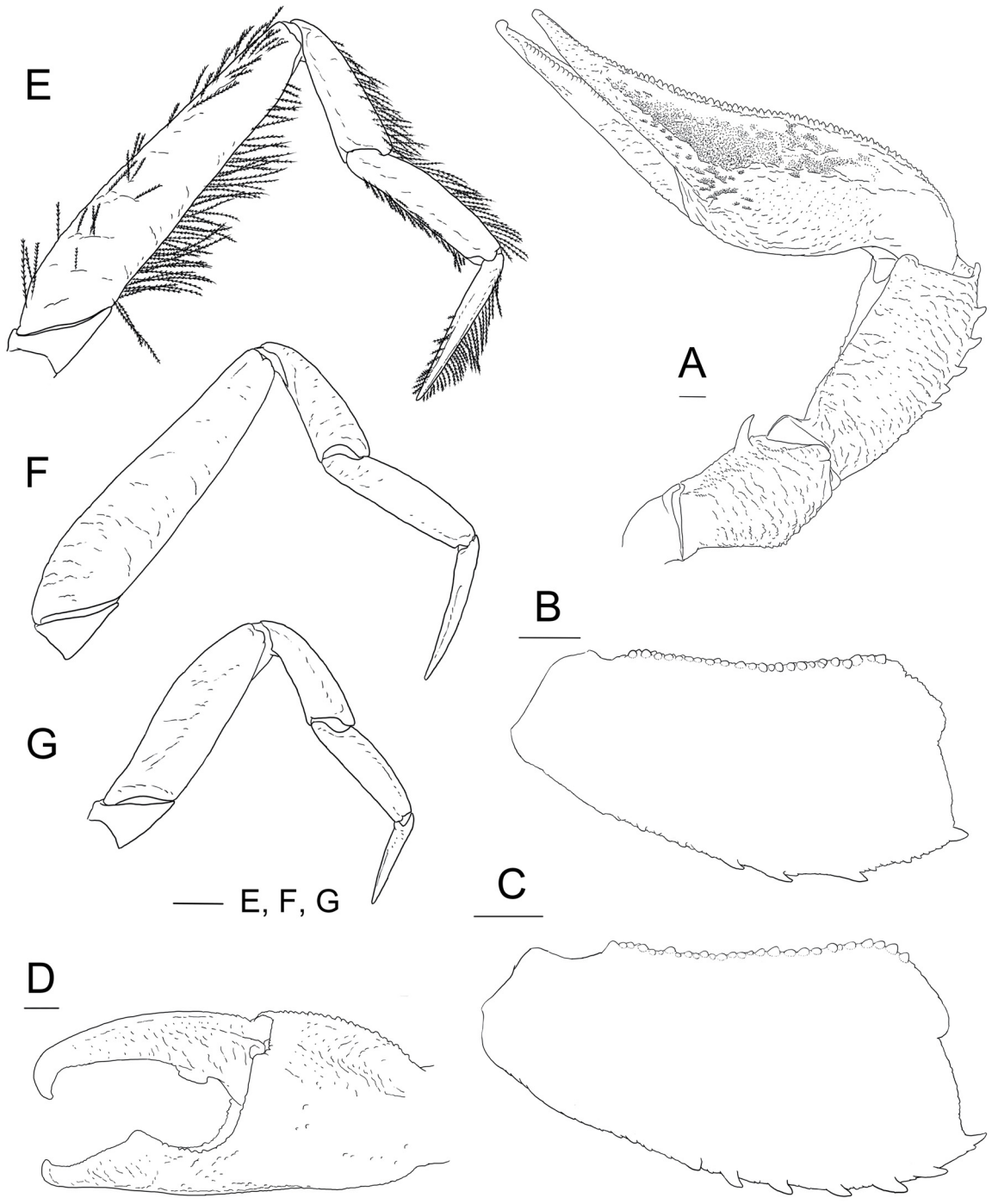

Fig. 6. *Raphidopus ciliatus* Stimpson, 1858. **A, D–G**. ♂, 10.2 mm (MBM287965), Hong Kong, China. **B**. ♂, (MBM287970), Danzhou, China. **C**. ♂, (MBM287968), Beihai, China. **A**. Larger cheliped, ventral view. **B–C**. Larger cheliped carpus, dorsal view. **D**. Larger chela, dorsal view. **E**. Right first ambulatory leg (with setae), lateral view. **F**. Right second ambulatory leg, lateral view. **G**. Right third ambulatory leg, lateral view. Scale bars = 1.0 mm.

margin of carpus; dorsodistal margin straight; ventral surface mesially with strong subterminal spine. Carpus distinctly elongate, 2.1 (2.0–2.2) times as long as broad, proximally narrowed; dorsoflexor margin slightly concave, bearing granules generally linearly arranged (few granules may present ventrally), granules bead-like (rarely tubercle-like), subequal in size and closely-spaced; extensor margin evenly convex, with 4–7 strong spines (including spine at distal end) on distal two-third; dorsodistal and ventrodistal margins sinuous; dorsal surface with longitudinal ridge on midline; dorsal and ventral surfaces with numerous short rugae. Palm compressed dorsoventrally, 1.1 times as long as broad, 0.9 times length of carpus; chela (including fingers) 2.6 (2.5–3.0) times as long as broad, 1.4 (1.3–1.8) times carapace width; extensor margin denticulate; dorsoflexor margin with row of beaded granules; dorsal surface with elevate longitudinal ridge on midline, with clusters of beaded granules along mid-ridge and numerous granules on extensor side; ventral surface with numerous rugae and distinct groove or depressed area along extensor margin extending onto base of fixed finger. Fingers approximately 1.2 times palm length, tips hooked and crossed to each other distally; dorso-extensor margin of dactylus ridged with beaded granules; dorsal surface of dactylus ridged on midline covered with beaded granules, dorsal and ventral surfaces of both fingers covered with short rugae; occlusal edges of larger chela with broad and triangular median tooth on fixed finger and produced, rectangular basal tooth on dactylus; occlusal edges of smaller chela straight and crenulate. Chela of larger male individuals usually less granulate.

Ambulatory legs. Each article compressed, with no spine and bearing thick plumose setae on margins and few short setae on surfaces. Meri slender, subequal in width and decreasing in length posteriorly; P2 merus 4.5 (4.3–4.7) times as long as broad, P3 and P4 meri approximately 0.8 and 0.5 times length of P2 merus, respectively; extensor and flexor margins generally straight. Carpi subequal in width; P2 carpus approximately 0.4 times length of P2 merus, 2.9 times as long as broad, P3 and P4 carpi 0.9 and 0.8 times length of P2 carpus, respectively; extensor and flexor margins straight. Propodi subequal in width, P2 propodus approximately 0.4 times length of merus, 4.1 times as long as broad, P3 and P4 propodi approximately 0.9 and 0.7 times length of P2 propodus, respectively; extensor margin slightly convex; flexor margin straight. Dactyli gradually narrowed distally, approximately 0.8–0.9 times length of propodi; extensor and flexor margins straight.

Pleopods. Males with pair of well-developed pleopods modified as gonopods on second abdominal somite. Females with pair of slender pleopods on each third to fifth abdominal somites.

Coloration in life

Body generally pale whitish. Anterior part of carapace and dorsal surfaces of chelipeds with purple patches. Plumose setae brown or black.

Habitat

Muddy and sandy-muddy substrates in the subtidal zones.

Distribution

West Pacific: northern South China Sea, Japan, Thailand, Malaysia Peninsula, Indonesia, northwest and east coasts of Australia; Indian Ocean: Pakistan; intertidal to depth of 44 m.

Remarks

Raphidopus ciliatus is closely related to *R. xinzhengi* sp. nov. (see Remarks on *R. xinzhengi*). Stimpson's (1858) original description of the holotype lacks details of the spination and granulation on the P1 carpus (Stimpson 1858, 1907). Measurements taken from the figure of the holotype (Stimpson 1907) give a P1 carpus length/width ratio of 2.1 and a chela-length/carapace-width ratio of 1.4; these values are close

to those of our *R. ciliatus* material herein defined. Meanwhile, the P1 carpus of the holotype seemed to have prominent spines on the extensor margin, contrasting with the small spines in the new species. We re-examined a syntype (see Supp. file 1) deposited in the Nature History Museum (NHM) in London (Reg. no. 61.44; pers. com., Dr Paul Clark) (Evans 1967). The syntype was collected from China, but no specific locality and date (with the label only reading "China (111)") were provided. The specimen shows sharp spines along the extensor margin and approximately linearly arranged granules on the dorsoflexor margin of the P1 carpus. Both the P1 carpus and chela are distinctly elongate, with length/width ratios of 3.0 and 2.2, respectively. Although all ambulatory legs are detached, the longest one also displays a markedly elongate merus (length/width ratio, 5.0). These characters are consistent with those of our specimens of *R. ciliatus*.

In Chinese waters, *R. ciliatus* predominates in the northern South China Sea and southern East China Sea (south to the northern end of the Taiwan Strait), whereas *R. xinzhengi* sp. nov. occurs exclusively north of the Taiwan Strait (according to our surveys). Examination of more than 15 specimens, including eight from adjacent waters of Hong Kong, confirms that populations across the northern South China Sea are morphologically and genetically uniform, indicating they are conspecific. Some intraspecific variations are observed in *R. ciliatus*: specimens from Guangdong and Hong Kong usually bear dark grey to black plumose setae, whereas specimens from the Beibu Gulf have dark brown setae.

Raphidopus ciliatus has been recorded widely from the Indo-West Pacific, including Pakistan, Australia, Japan, Indonesia and Malaysia (Miyake 1943; Haig 1965, 1981; Ng & Nakasone 1994; Tirmizi & Ghani 1994), demonstrating a wide distribution range throughout the tropical Indo-West Pacific. Miyake (1943) illustrated a specimen from Japan with a somewhat long P1 carpus (length/width ratio roughly 1.9–2.0), bearing strong spines on the extensor margin, making it more similar to *R. ciliatus*. Specimens examined by Haig (1992) and Ng & Nakasone (1994) exhibited a much more elongate P1 carpus that agrees well with our material. Tirmizi & Ghani's (1994) material from Pakistan, by contrast, has a relatively short P1 carpus and a degree of variation on the spination of the carapace. Given the high morphological similarity, yet strong genetic divergence between *R. ciliatus* and *R. xinzhengi* sp. nov., a molecular analysis and re-examination of *R. ciliatus* material from the other geographical regions will be required to clarify their systematic status and the true distribution range.

Raphidopus xinzhengi Dong, Wan & Wang sp. nov.
urn:lsid:zoobank.org:act:A5A94BE4-5BF0-4800-9550-93AFDFD2A087
Figs 1–3, 4B, 7–8

Raphidopus ciliatus – Kim & Kim 2017: 87, fig. 40.

Diagnosis

Carapace broader than long, lateral margins with 3 or 4 spines; hepatic margin separated from branchial margin by fissure or narrow V-shaped notch; dorsal surface with pair of oblique posterolateral ridges each unarmed or with 1 (rarely 2) small spines. Median lobe of thoracic sternite 3 comparatively high antero-posteriorly. Cheliped bearing long and thick plumose setae on margins and surfaces of all articles; carpus moderately elongate, 1.8–1.9 times as long as broad; dorsoflexor margin bearing granules arranged in irregular rows, granules bead-like or tubercle-like, generally irregular in size and spacing; extensor margin with 3–5 small spines; chela 2.2–2.4 times as long as broad, 1.0–1.3 times carapace width; palm with longitudinal groove on ventral surface near extensor margin. Ambulatory legs bearing long plumose setae; merus of second ambulatory leg 3.4–3.8 times as long as broad.

Etymology

The new species is named after Professor Xinzheng Li, Institute of Oceanology, Chinese Academy of Sciences, for his contribution to the taxonomic research of marine crustaceans in China. The Chinese name of the new species is 新正细足蟹.

Type material

Holotype

CHINA – **Yellow Sea** • ♀ (CL 8.3 mm); Shandong Province, Jiaozhou Bay, Qingdao; 36°09′ N, 120°20′ E; 5 m depth; 10 Nov. 2024; collected by dredge, muddy bottom; GenBank no.: PX405584; MBM287959.

Paratypes

CHINA – **Yellow Sea** • 2 ♀♀ (CL 4.5–6.6 mm), 2 ♂♂ (CL 6.2–7.5 mm); Shandong Province, Dingzi Bay, Haiyang, Yantai; 36°35′ N, 120°59′ E; 6 m depth; 17 Apr. 2022; collected by bottom trawl; GenBank no.: PX405585; MBM287960.

Non-type material examined

CHINA – **East China Sea** • 2 ♀♀ (CL 5.1–7.4 mm), 4 ♂♂ (CL 5.4–8.2 mm); Zhejiang Province, Nanji Islands, Wenzhou; 27°27′ N, 121°5′ E; 2 Jun. 2022; collected by bottom trawl; MBM287962. – **Yellow Sea** • 1 ♀ (CL 6.1 mm), 1 ♂ (CL 8.1 mm); Liaoning Province, Liaodong Bay, Panjin; 40°33′ N, 121°56′ E; 1 Nov. 2024; collected by bottom trawl; GenBank no.: PX405586; MBM287963 • 4 ♀♀ (CL 5.5–8.0 mm), 2 ♂♂ (CL 7.5–8.5 mm); Shandong Province, Jiaozhou Bay, Qingdao; 36°09′ N, 120°20′ E; 5 m depth; 11 Feb. 2017; collected by dredge, muddy bottom; MBM287961 • 4 ♀♀ (CL 7.1–8.0 mm), 2 ♂♂ (CL 8.0–9.3 mm); Jiangsu Province, Ganyu, Lianyungang; 35°2′ N, 119°18′ E; 10 m depth; 8 Apr. 2024; collected by bottom trawl; MBM287964.

Description

Carapace. 1.3 (1.2–1.3) times as broad as broad; lateral margins strongly convex. Dorsal surface finely covered with numerous short striae, striae relatively long and elevated on lateral branchial and intestinal regions and usually bearing dense plumose setae; gastric and cardiac regions relatively glabrous or with sparse short setae, pair of protogastric ridges present; cervical grooves distinct. Hepatic margin convex, separated from branchial margin by fissure or narrow V-shaped notch. Branchial margins strongly convex, tuberculate, laterally expanded forming laminar ridges convergent posteriorly, armed with 3 or 4 small spines, oblique posterolateral ridge crenulate, extending onto posterior branchial region, unarmed or bearing 1 (rarely 2) small median spines. Posterior margin slightly concave. Rostrum short, trilobate; median lobe broad, bent ventrally, with short dorsomedian groove; lateral lobe approximately as broad as median lobe, half of median lobe length. Orbit concave; supra-ocular margins smooth; outer orbital angles bluntly triangular, approximately reaching half length of lateral rostral lobe. Pterygostomian flap entire; surface with longitudinal, long ridge on midline and several short, oblique rugae bearing thick plumose setae; anterior end produced, triangular.

Sternal plastron. Sternite 3 broad; median lobe trilobate, approximately 3.5 times as wide as high (width measured along anterior margin of sternite 3 excluding elongated lateral lobes), anterior margin transversely straight or slightly convex; lateral lobes narrow, strongly produced anteriorly reaching half length of coxa of third maxilliped. Sternite 4 with anterior margin concave, bearing submarginal row of thick plumose setae.

Telson. Composed of 7 plates.

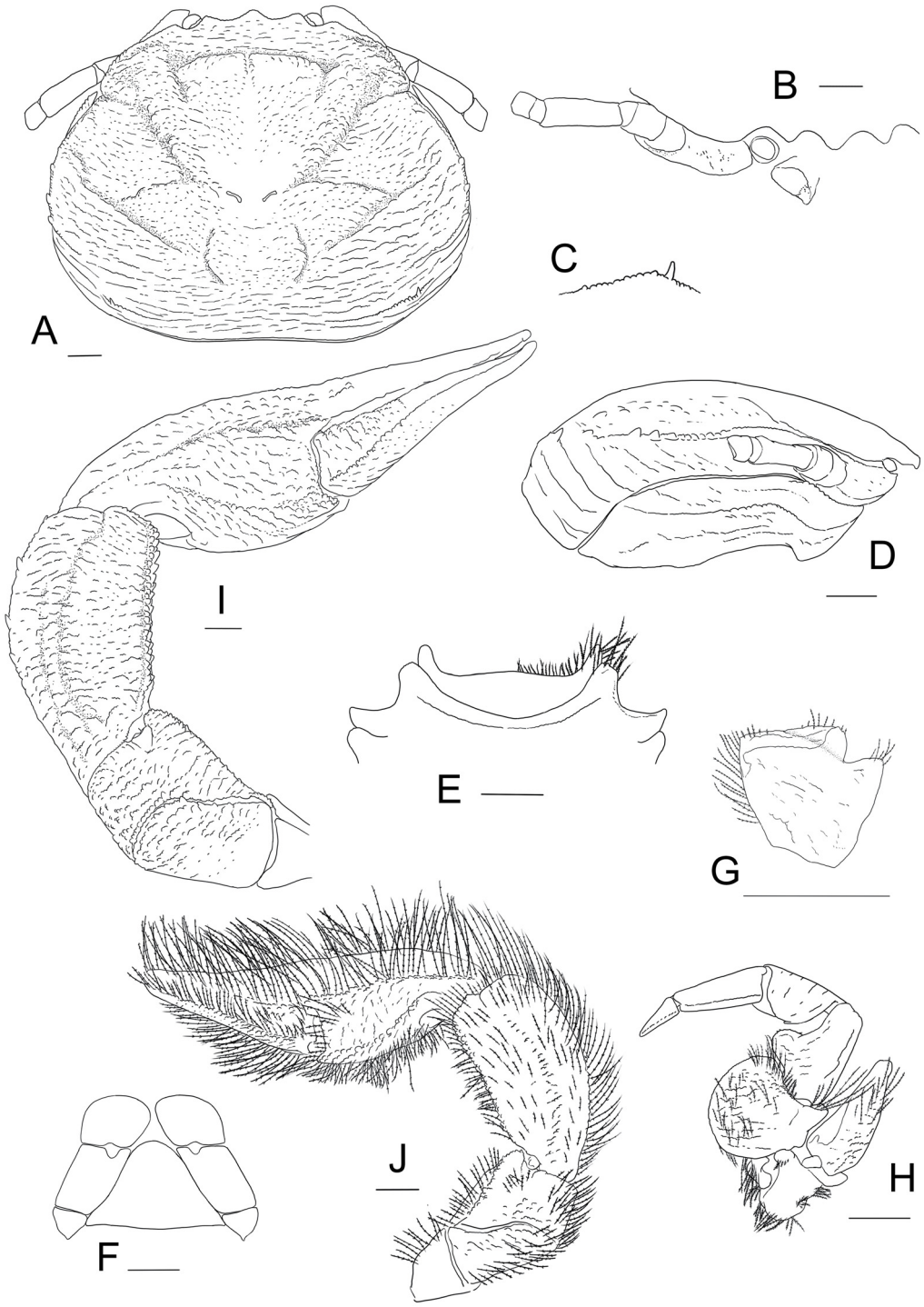

Fig. 7. *Raphidopus xinzhengi* Dong, Wan & Wang sp. nov., holotype, ♀, 8.3 mm (MBM287959), Jiaozhou Bay, Qingdao, China. **A**. Carapace, dorsal view. **B**. Right antennal peduncles and basal article of antennular peduncle, dorsolateral view. **C**. Posterolateral ridge of carapace. **D**. Right carapace and pterygostomian, lateral view. **E**. Third and fourth thoracic sternites (setae partially shown), ventral view. **F**. Telson, external view. **G**. Basal article of right antennular peduncle (with setae), ventral view. **H**. Left third maxilliped (setae partially shown), lateral view. **I**. Larger cheliped, dorsal view. **J**. Smaller cheliped (with setae), dorsal view. Scale bars = 1.0 mm.

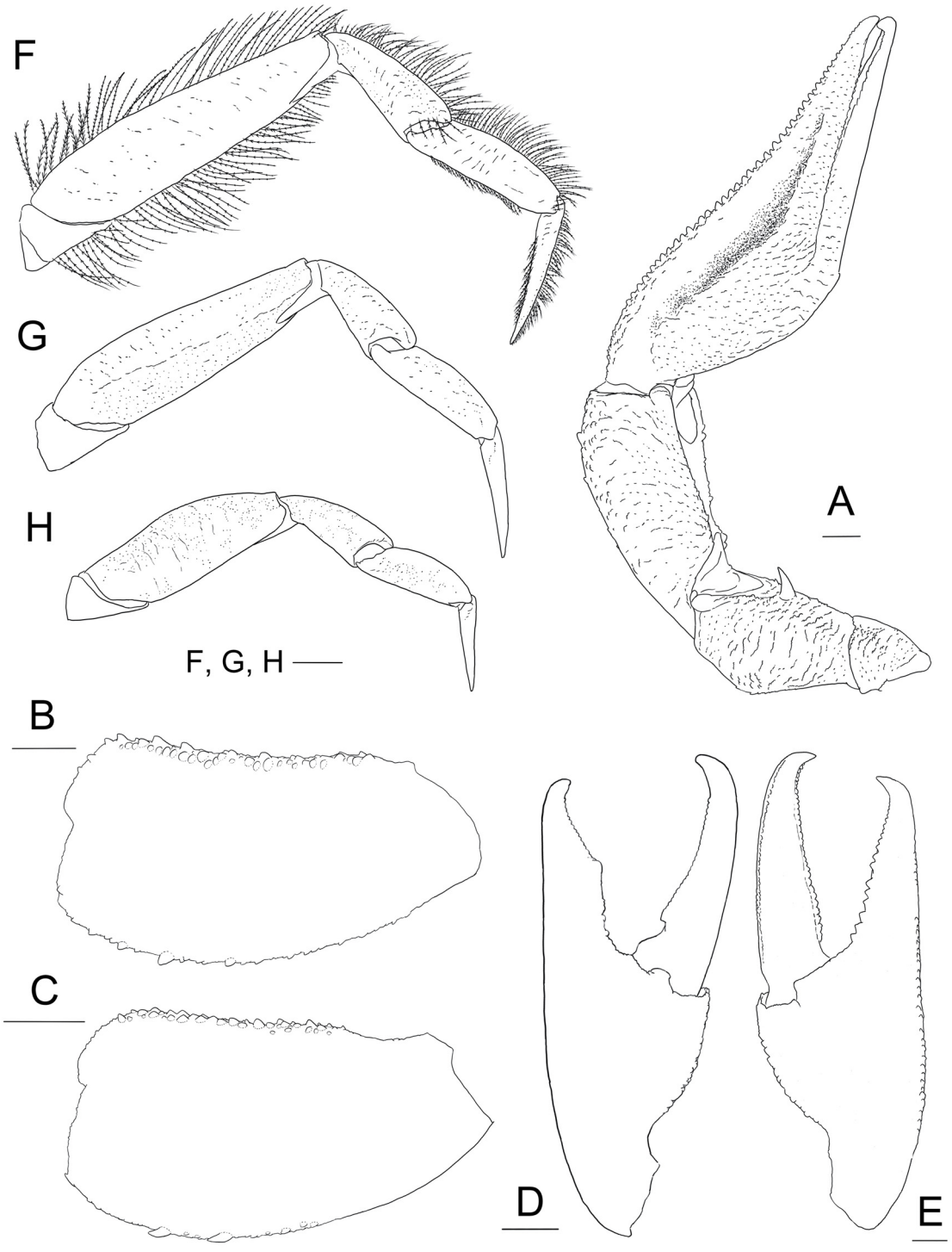

Fig. 8. *Raphidopus xinzhengi* Dong, Wan & Wang sp. nov. **A, D–H**. Holotype, ♀, 8.3 mm (MBM287959), Jiaozhou Bay, Qingdao, China. **B**. ♂, 8.1 mm (MBM287963), Panjin, China. **C**. ♀, (MBM287964), Lianyungang, China. **A**. Smaller cheliped, ventral view. **B–C**. Larger cheliped carpus, dorsal view. **D**. Larger chela, dorsal view. **E**. Smaller chela, dorsal view. **F**. Right first ambulatory leg (with setae), lateral view. **G**. Right second ambulatory leg, lateral view. **H**. Right third ambulatory leg, lateral view. Scale bars = 1.0 mm.

Eye. Small, ocular peduncle short, distal margin of cornea reaching apex of lateral rostral lobe.

Basal article of antennular peduncle. As long as or slightly longer than broad, with short transverse rugae on ventral surface; anterior margin crenulate, mesial corner elevated and produced as rounded tooth.

Antenna1 peduncle. First article immovable, broad, anteriorly reaching level of cornea; second to fourth articles movable, subcylindrical, unarmed, third article longest.

Third maxilliped. Ischium rounded and lamellar, lateral surface medially depressed, with transverse rugae bearing short plumose setae. Merus with rounded lobe on flexor margin; extensor margin straight; lateral surface with short rugae. Carpus with rounded projection on median flexor margin. Propodus straight, elongate. Dactylus short.

Cheliped (pereopod 1; P1). Unequal, bearing long and thick plumose setae on margins and surfaces of all articles, setae especially thicker on extensor and flexor margins of each article, ventral surface of merus and dorsal surface of chela. Merus robust, longer than broad, surfaces covered with numerous short rugae; dorsoflexor lobe low, marginally granulate, distally rounded and overreaching proximal margin of carpus; dorsodistal margin straight; ventral surface distally with strong subterminal spine. Carpus moderately elongate, 1.9 (1.8–1.9) times as long as broad, proximally narrowed; dorsoflexor margin generally straight, bearing granules arranged in irregular rows, granules bead-like or tubercle-like, generally irregular in size and spacing; extensor margin convex, rounded, with 3–5 small or tubercle-like spines on distal half, spine at distal end sometimes absent; dorsodistal and ventrodistal margins sinus; dorsal surface with longitudinal ridge on midline; dorsal and ventral surfaces with numerous scattered, short rugae. Palm compressed dorsoventrally, approximately 1.1 times as long as broad, 0.9 times length of carpus; chela (including fingers) 2.3 (2.2–2.4) times as long as broad, 1.2 (1.0–1.3) times carapace width; extensor margin denticulate; dorsoflexor margin with row of beaded granules; dorsal surface ridged on midline, with clusters of beaded granules along mid-ridge and numerous granules on extensor side; ventral surface with numerous rugae and distinct groove or depressed area near extensor margin extending onto mid-length of fixed finger. Fingers approximately 1.1 times as long as palm, tips hooked, crossed to each other distally; dorso-extensor margin of dactylus ridged with beaded granules; dorsal and ventral surfaces of both fingers covered with short rugae; occlusal edges in larger chela with broad, triangular median tooth on fixed finger and produced, triangular basal tooth on dactylus; occlusal edges in smaller chela straight, each with row of small teeth. Dorsal surfaces of palm and fingers usually less granulate or smooth in large male individuals.

Ambulatory legs (pereopods 2–4; P2–4). Each article mesio-laterally compressed, without spine but bearing thick plumose setae on margins and few short setae on surfaces. Meri slender, subequal in width but decreasing in length posteriorly; P2 merus 3.6 (3.4–3.8) times as long as broad, P3 and P4 merus approximately 0.9 and 0.6 times length of P2 merus, respectively; extensor and flexor margins generally straight. Carpi subequal in width; P2 carpus approximately 0.4 length of merus, 2.4 times as long as broad, P3 and P4 carpi approximately 0.8 times length of P2 carpus; extensor and flexor margins straight. Propodi subequal in width, P2 propodus approximately half length of P2 merus, 3.1 times as long as broad, P3 and P4 propodi 0.9 and 0.7 times length of P2 propodus, respectively; extensor margin slightly convex; flexor margin straight. Dactyli gradually narrowed distally, approximately 0.8–0.9 times length of propodi; extensor and flexor margins straight.

Pleopods. Males with pair of well-developed pleopods modified as gonopods on second abdominal somite. Females with pair of slender pleopods on each third to fifth abdominal somites.

Coloration in life

Carapace generally brown and white. Anterior part of carapace and dorsal surfaces of chelipeds with blue or purple patches. Plumose setae light brown.

Habitat

Muddy and sandy-muddy bottoms of subtidal and lower intertidal zones.

Distribution

Northern Chinese coastal waters (north of the Taiwan Strait), the Korean Peninsula; intertidal to depths 30 m.

Remarks

Raphidopus xinzhengi sp. nov. is morphologically most similar to *R. ciliatus* in having the following characters: the carapace branchial margin has spines and is separated from the hepatic margin by a narrow notch, and the P1 carpus has a row of spines on the extensor margin and a longitudinal ridge on the midline of the dorsal surface. The new species, however, differs from *R. ciliatus* by the irregularly arranged granules on the dorsoflexor margin of P1 carpus, the comparatively shorter P1 carpus (1.8–1.9 times as long as broad; average 1.9, n = 10), P1 chela (1.0–1.3 times carapace width; average 1.2, n = 10) and P2 merus (3.4–3.8 times as long as broad; average 3.6, n = 10). Additionally, the granules on the dorsoflexor margin of P1 carpus in the new species are generally variable in size, shape and spacing, and are not linearly arranged. While in *R. ciliatus*, the P1 carpus (2.0–2.2 times as long as broad; average 2.1, n = 10), the P1 chela (1.3–1.8 times the carapace width; average 1.4, n = 10) and the P2 merus (4.3–4.7 times as long as broad; average 4.5, n = 10) are much elongated; especially the granules on the P1 carpus are generally uniform in size and evenly spaced, and arranged linearly. In addition, the new species has no spine or comparatively short, reduced spine(s) on the posterolateral ridges of the carapace and short spines on the extensor margin of the P1 carpus. The posterolateral ridge of the carapace is unarmed on nearly half of the individuals examined, and the spine at the distal end of the extensor margin of P1 carpus is usually absent.

The new species also resembles *R. dhritiae* in the armature of the carapace and chelipeds, and the size of the P1 carpus and P2 merus. The new species differs from *R. dhritiae* in having a fissure or narrow V-shaped notch between the hepatic and branchial margins, no spine or a single (rarely two) small spine on the posterolateral ridge of the carapace, comparatively narrower antennular basal article (as long as broad), and a broad median tooth on the occlusal edge of the P1 fixed finger; whereas in *R. dhritiae*, there is a broader U-shaped notch between the hepatic and branchial margins, two distinct spines on the posterolateral ridge of the carapace, a much broader antennular basal article, and two broad teeth (subproximal and distal) on the occlusal edge of the P1 fixed finger. In addition, according to the illustration by Mitra *et al.* (2024), the thoracic sternite 3 of *R. dhritiae* is comparatively lower antero-posteriorly than those in *R. xinzhengi* sp. nov. and *R. ciliatus*.

Both *R. xinzhengi* sp. nov. and *R. ciliatus* have a longitudinal groove or depressed area on the extensor side of the ventral surface of the P1 palm, a significant feature that readily distinguishes the two species from other tropical Indo-Pacific species such as *R. indicus*, *R. brevipes* and *R. johnsoni* (Osawa & Ng 2018). This character, however, is undocumented in *R. persicus* and *R. dhritiae*.

Based on our surveys and sampling, the distribution of *R. xinzhengi* sp. nov. is restricted to waters north of the Taiwan Strait; therefore, it should be endemic to the marginal seas of the northwest Pacific, including the East China Sea and Yellow Sea The specimens reported by Kim & Kim (2017) from the Deuk-Ryang Bay, South Korea, exhibit short P1 carpus, consistent with the characters observed in the

new species. The current records indicate that the species occurs exclusively in the northern waters of the West Pacific.

Key to species of Raphidopus Stimpson, 1858 (modified from Osawa & Ng 2018)

1. Branchial margins of carapace with distinct spines 2
– Branchial margins of carapace without spines 4

2. Branchial margin and hepatic margin of carapace separated by broad U-shaped notch .... ***R. dhritiae*** Mitra, Chowdhury & Bose, 2024
– Branchial margin and hepatic margin of carapace separated by fissure or narrow V-shaped notch 3

3. Dorsoflexor margin of P1 carpus with irregularly arranged granules; P1 carpus less than 2 times as long as broad, P2 merus less than 4.0 times as long as broad .... ***R. xinzhengi*** Dong, Wan & Wang sp. nov.
– Dorsoflexor margin of P1 carpus with linearly and regularly arranged granules; P1 carpus at least 2 times as long as broad, P2 merus more than 4.0 times as long as broad .... ***R. ciliatus*** Stimpson, 1858

4. P1 carpus with 3 or 4 sharp spines on distal third of posterior margin .... ***R. persicus*** Ng, Safaie & Naser, 2012
– P1 carpus unarmed on posterior margins 5

5. P1 carpus usually with blunt longitudinal ridge on midline of dorsal surface. Dactylus of larger cheliped with 2 distinct proximal teeth on cutting edge. Ambulatory legs comparatively stout (in fourth pereopod, 2.4–2.6 and 2.2–2.4 times as long as high on merus and propodus, respectively) .... ***R. brevipes*** Osawa & Ng, 2018
– Carpus of each cheliped without blunt longitudinal ridges on midline of dorsal surface. Dactylus of larger cheliped with 1 distinct proximal tooth on cutting edge. Ambulatory legs slender (in fourth pereopod, 2.8–3.1 and 2.7–3.0 times as long as high on merus and propodus, respectively) 6

6. Eyes comparatively large, reaching lateral limits of orbits. Dactylus of larger cheliped with distinct, blunt tooth on median part of cutting edge, in addition to 1 proximal tooth .... ***R. johnsoni*** Ng & Nakasone, 1994
– Eyes small, not reaching lateral limits of orbits. Dactylus of larger cheliped without prominent tooth on median part of cutting edge ..... ***R. indicus*** Henderson, 1893

Discussion

The mitochondrial COI gene is widely used as a barcoding marker for species delimitation in crustaceans and many other invertebrate groups (Hebert *et al.* 2003). The generally accepted threshold for species delimitation in crustaceans is 3% for the COI gene (Lefébure *et al.* 2006; Rodríguez-Flores *et al.* 2019). Hiller & Werding (2022) reported an interspecific distance of 6.2% between congeneric porcellanids *Porcellana platycheles* (Pennant, 1777) and *P. africana* Chace, 1956. The interspecific genetic distance between *R. xinzhengi* sp. nov. and *R. ciliatus* was found to be 8.7–9.0%, substantially higher than the intraspecific genetic variation within each species (≤ 0.4%), supporting the independent status of the new species.

Both the phylogenetic tree and the haplotype network revealed congruent lineage structures, showing that *R. xinzhengi* sp. nov. and *R. ciliatus* constitute two distinct species. The haplotypes of the two species are separated by at least 46 mutational steps, forming two distinctly separate clusters with no shared or intermediate haplotypes. This aligns with findings from studies on other porcellanid species complex,

where cryptic species, despite high morphological similarity, have haplotypes separated from their sister species by substantial mutations (Fang *et al.* 2023).

The discovery of *R. xinzhengi* sp. nov. contributes to the known diversity of the genus *Raphidopus*. Geographically, *R. xinzhengi* inhabits the northern coastal waters of China, including the Yellow Sea and East China Sea. In contrast, *R. ciliatus* is restricted to the southern waters south of the Taiwan Strait. The two species seem to exhibit an allopatric distribution along the Chinese mainland coast, with no distinct overlapping zones identified in our sampling; however, further surveys are needed to confirm this spatial pattern.

The Taiwan Strait has been identified as a significant phylogeographic barrier for many marine invertebrates. Studies on species such as the bivalve *Meretrix petechialis* (Lamarck, 1818), and the decapod crustaceans *Tubuca arcuata* (De Haan, 1835) and *Eriocheir* s. str. (Xu *et al.* 2009; Wang *et al.* 2017; Shih *et al.* 2022) have demonstrated restricted dispersal across this region. It is widely held that the emergence of a land bridge across the Taiwan Strait during glacial periods promoted the divergence between populations in the East and South China Seas (e.g., Shih *et al.* 2022). On the other hand, an asymmetrical gene flow has been observed between the two sides of the strait, indicating that ocean currents also serve as a key factor limiting dispersal across the strait (Fang *et al.* 2023). Therefore, the current phylogeographical patterns of the two species of *Raphidopus* are likely shaped by a combination of historical geological events and contemporary oceanographic factors.

Acknowledgments

This study was financially supported by the Biological Resources Program, Chinese Academy of Sciences (CAS-TAX-24-029). We are deeply grateful to Dr Paul F. Clark of the NHM for his assistance in locating the syntype of *R. ciliatus* and providing us with the valuable photographs of the specimen.

References

Burland T.G. 2000. DNASTAR's lasergene sequence analysis software. *Methods in Molecular Biology* 132: 71–91. https://doi.org/10.1385/1-59259-192-2:71

Dong D., Xu P., Li X. & Wang C. 2019. *Munidopsis* species (Crustacea: Decapoda: Munidopsidae) from carcass falls in Weijia Guyot, West Pacific, with recognition of a new species based on integrative taxonomy. *PeerJ* 7: e8089. https://doi.org/10.7717/peerj.8089

Evans A.C. 1967. Syntypes of Decapoda described by William Stimpson and James Dana in the collections of the British Museum (Natural History). *Journal of Natural History* 1 (3): 399–411. https://doi.org/10.1080/00222936700770391

Fang X., Dong D., Yang M. & Li X. 2023. Phylogenetics and population genetics of the *Petrolisthes lamarckii–P. haswelli* complex in China: Old lineage and new species. *International Journal of Molecular Sciences* 24 (21): 15843. https://doi.org/10.3390/ijms242115843

Folmer O., Black M., Hoeh W., Lutz R. & Vrijenhoek R. 1994. DNA primers for amplification of mitochondrial cytochrome C oxidase subunit I from diverse metazoan invertebrates. *Molecular Marine Biology and Biotechnology* 3: 294–299.

Grant F.E. & McCulloch A.R. 1906. On a collection of Crustacea from the Port Curtis District, Queensland. *Proceedings of the Linnean Society of New South Wales* 31: 2–53.

Haig J. 1965. The Porcellanidae (Crustacea, Anomura) of Western Australia), with descriptions of four new Australian species. *Journal of the Royal Society of Western Australia* 48 (4): 97–118.

Haig J. 1966. The Porcellanidae (Crustacea Anomura) of the Iranian Gulf and Gulf of Oman. *Videnskabelige Meddelelser Dansk Naturhistrisk Forening i Kjøbenhavn* 129: 49–65.

Haig J. 1981. Porcellanid crabs from the Indo-west Pacific, Part II. *Steenstrupia* 7: 269–291.

Haig J. 1992. Hong Kong's porcellanid crabs. *In*: Morton B. (ed.) *The Marine Flora and Fauna of Hong Kong and Southern China III*: 303–327. Hong Kong University Press, Hong Kong.

Hebert P.D.N., Ratnasingham S. & de Waard J.R. 2003. Barcoding animal life: Cytochrome c oxidase subunit 1 divergences among closely related species. *Proceedings of the Royal Society B: Biological Sciences* 270 (suppl_1): S96–S99. https://doi.org/10.1098/rsbl.2003.0025

Henderson J.R. 1888. Report on the Anomura collected by H.M.S Challenger during the years 1873–1876. *In*: Murray J. (ed.) *Zoology. Report on the Scientific Results of the Voyage of H.M.S. Challenger During the Years 1873–76 Under the Command of Captain George S. Nares, R.N., F.R.S. and the Late Captain Frank Tourle Thomson, R.N. Wyville Thomson, C. and J. Murray (series eds.)* Vol. 27: i–xi, 1–221. Neill and Company, Edinburgh. https://doi.org/10.5962/bhl.title.6513

Henderson J.R. 1893. A contribution to Indian carcinology. *Transactions of the Linnean Society of London, Series 2, Zoology* 5 (10): 325–458. https://doi.org/10.1111/j.1096-3642.1893.tb00653.x

Hiller A. & Werding B. 2022. Multigene phylogeny of the Indo-west Pacific genus *Enosteoides* (Crustacea, Decapoda, Porcellanidae) with description of a new species from Australia. *Zoosystematics and Evolution* 98 (2): 387–397. https://doi.org/10.3897/zse.98.90540

Hsieh B.-F., Chan T.-Y. & Yu H.-P. 1997. On the porcellanid crabs (Crustacea: Decapoda: Porcellanidae) of Taiwan. *Annals of the Taiwan Museum* 40: 275–359.

Kalyaanamoorthy S., Minh B.Q., Wong T.K.F., von Haeseler A. & Jermiin L.S. 2017. ModelFinder: Fast model selection for accurate phylogenetic estimates. *Nature Methods* 14 (6): 587–589. https://doi.org/10.1038/nmeth.4285

Kim J.N. & Kim M.Y. 2017. Hermit crabs II: Arthropoda: Malacostraca: Decapoda: Axiidae, Callianassidae, Upogebiidae, Hapalogastridae, Lithodidae, Diogenidae, Paguridae, Pylochelidae, Chirostylidae, Galatheidae, Munididae, Porcellanidae, Blepharipodidae. *Invertebrate Fauna of Korea* 21 (43): 1–113. National Institute of Biological Resources, Incheon.

Kimura M. 1980. A simple method for estimating evolutionary rates of base substitutions through comparative studies of nucleotide sequences. *Journal of Molecular Evolution* 16 (2): 111–120. https://doi.org/10.1007/BF01731581

Kumar S., Stecher G. & Tamura K. 2016. MEGA7: Molecular Evolutionary Genetics Analysis version 7.0 for bigger datasets. *Molecular Biology and Evolution* 33 (7): 1870–1874. https://doi.org/10.1093/molbev/msw054

Lefébure T., Douady C.J., Gouy M. & Gibert J. 2006. Relationship between morphological taxonomy and molecular divergence within Crustacea: Proposal of a molecular threshold to help species delimitation. *Molecular Phylogenetics and Evolution* 40 (2): 435–447. https://doi.org/10.1016/j.ympev.2006.03.014

Leigh J.W. & Bryant D. 2015. Popart: Full-feature software for haplotype network construction. *Methods in Ecology and Evolution* 6 (9): 1110–1116. https://doi.org/10.1111/2041-210X.12410

Letunic I. & Bork P. 2021. Interactive tree of life (iTOL) v5: An online tool for phylogenetic tree display and annotation. *Nucleic Acids Research* 49 (W1): W293–W296. https://doi.org/10.1093/nar/gkab301

Mitra S., Chowdhury P. & Bose M. 2024. *Raphidopus dhritiae* sp. nov. (Decapoda: Anomura: Porcellanidae) from Matla River Bank of Canning, West Bengal, India. *Records of Zoological Survey of India* 124: 13–20. https://doi.org/10.26515/rzsi/v124/i1S/2024/172711

Miyake S. 1943. Studies on the crab-shaped Anomura of Nippon and adjacent waters. *Journal of the Department of Agriculture, Kyushu Imperial University* 7: 49–158.

Ng P.K.L. & Nakasone Y. 1994. On the porcellanid genera *Raphidopus* Stimpson, 1858, and *Pseudoporcellanella* Sankarankutty, 1961, with description of a new mangrove species, *Raphidopus johnsoni* from Singapore (Decapoda, Anomura). *Crustaceana* 66 (1): 1–21. https://doi.org/10.1163/156854094X00116

Ng P.K.L., Safaie M. & Naser M.D. 2012. A new species of *Raphidopus* Stimpson, 1858, from the Persian Gulf (Crustacea: Decapoda: Anomura: Porcellanidae). *Zootaxa* 3402 (1): 54–60. https://doi.org/10.11646/zootaxa.3402.1.4

Nguyen L.-T., Schmidt H.A., von Haeseler A. & Minh B.Q. 2015. IQ-TREE: A fast and effective stochastic algorithm for estimating maximum-likelihood phylogenies. *Molecular Biology and Evolution* 32 (1): 268–274. https://doi.org/10.1093/molbev/msu300

Osawa M. & Chan T.-Y. 2010. Part III. Porcellanidae (Porcelain crabs). *In*: Chan T.-Y. (ed.) *Crustacean Fauna of Taiwan: Crab-like Anomurans (Hippoidea, Lithodoidea and Porcellanidae)*: 67–181. National Taiwan Ocean University Press, Keelung.

Osawa M. & Ng P.K.L. 2018. A new species of the genus *Raphidopus* Stimpson, 1858 (Crustacea: Decapoda: Anomura: Porcellanidae) from Peninsular Malaysia, with additional records of *R. johnsoni* Ng & Nakasone, 1994 from Southeast Asia, and a key to species in the genus. *Zootaxa* 4433 (1): 111–126. https://doi.org/10.11646/zootaxa.4433.1.6

Rodríguez-Flores P.C., Machordom A., Abelló P., Cuesta J.A. & Macpherson E. 2019. Species delimitation and multi-locus species tree solve an old taxonomic problem for European squat lobsters of the genus *Munida* Leach, 1820. *Marine Biodiversity* 49: 1751–1773. https://doi.org/10.1007/s12526-019-00941-3

Ronquist F., Teslenko M., van der Mark P., Ayres D.L., Darling A., Hohna S., Larget B., Liu L., Suchard M.A. & Huelsenbeck J.P. 2012. MrBayes 3.2: Efficient Bayesian phylogenetic inference and model choice across a large model space. *Systematic Biology* 61: 539–542. https://doi.org/10.1093/sysbio/sys029

Rozas J., Ferrer-Mata A., Sánchez-DelBarrio J.C., Guirao-Rico S., Librado P., Ramos-Onsins S.E. & Sánchez-Gracia A. 2017. DnaSP 6: DNA sequence polymorphism analysis of large data sets. *Molecular Biology and Evolution* 34 (12): 3299–3302. https://doi.org/10.1093/molbev/msx248

Schwarz G. 1978. Estimating the dimension of a model. *The Annals of Statistics* 6 (2): 461–464. https://doi.org/10.1214/aos/1176344136

Shih H.-T., Liu M.-Y., Aoki M. & Suzuki H. 2022. Phylogeography of the fiddler crab *Tubuca arcuata* (Crustacea: Brachyura: Ocypodidae) in East Asia and Northern Vietnam. *Zoological Studies* 61: e68. https://doi.org/10.6620/ZS.2022.61-68

Stimpson W. 1858. Prodromus descriptionis animalium evertebratorum, quae in expeditione ad oceanum pacificum septentrionalem, a republica federata missa, Cadwaladaro Ringgold et Johanne Rodgers ducibus, observavit et descripsit. Pars VII. Crustacea Anomura. *Proceedings of the Academy of Natural Sciences of Philadelphia* 10: 225–252. https://doi.org/10.5962/bhl.title.51447

Stimpson W. 1907. Report on the Crustacea (Brachyura and Anomura) collected by the North Pacific Exploring Expedition, 1853–1856. *Smithsonian Miscellaneous Collections* 49: 1–240. https://doi.org/10.5962/bhl.title.51448

Tirmizi N.M. & Ghani N. 1994. An Indian Ocean record for a porcellanid crab, *Raphidopus ciliatus* Stimpson, 1858. *Pakistan Journal of Marine Sciences* 3: 69–72.

Wang X., Kong L., Chen J., Matsukuma A. & Li Q. 2017. Phylogeography of bivalve *Meretrix petechialis* in the Northwestern Pacific indicated by mitochondrial and nuclear DNA data. *PLoS ONE* 12 (8): e0183221. https://doi.org/10.1371/journal.pone.0183221

Xu J., Chan T.-Y., Tsang L.M. & Chu K.H. 2009. Phylogeography of the mitten crab *Eriocheir sensu stricto* in East Asia: Pleistocene isolation, population expansion and secondary contact. *Molecular Phylogenetics and Evolution* 52 (1): 45–56. https://doi.org/10.1016/j.ympev.2009.02.007

Yang S. & Sun X. 1990. On the porcellanid crabs from the coast of Fujian Province, China. *Memoirs of Beijing Natural History Museum* 45: 1–15. [In Chinese.]

Yang S. & Sun X. 1992. On the porcellanid crab (Anomura: Porcellanidae) of Guangxi Province, China. *Transactions of the Chinese Crustacean Society* 3: 196–213. [In Chinese.]

Yang S. & Sun X. 2005. The Porcellanidae (Crustacea: Anomura) of Hainan Island, China with description of a new species. *Natural Sciences and Museums* 1 (1): 1–30.

Zhang D., Gao F., Jakovlić I., Zou H., Zhang J., Li W.X. & Wang G.T. 2020. PhyloSuite: An integrated and scalable desktop platform for streamlined molecular sequence data management and evolutionary phylogenetics studies. *Molecular Ecology Resources* 20 (1): 348–355. https://doi.org/10.1111/1755-0998.13096

Printed versions of all papers are deposited in the libraries of two of the institutes that are members of the *EJT* consortium: Muséum national d'Histoire naturelle, Paris, France and Royal Museum for Central Africa, Tervuren, Belgium. The other members of the consortium are: Royal Belgian Institute of Natural Sciences, Brussels, Belgium; Meise Botanic Garden, Meise, Belgium; Natural History Museum of Denmark, Copenhagen, Denmark; Naturalis Biodiversity Center, Leiden, the Netherlands; Museo Nacional de Ciencias Naturales-CSIC, Madrid, Spain; Leibniz Institute for the Analysis of Biodiversity Change, Bonn – Hamburg, Germany; National Museum of the Czech Republic, Prague, Czech Republic; The Steinhardt Museum of Natural History, Tel Aviv, Israël.

Supplementary file

Supp. file 1. Syntype of *Raphidopus ciliatus* Stimpson, 1858. (Reg. no. 61.44), collected from China, deposited in the NHM in London, dorsal view. Photographed by Peter Grugeon, NHM Publishing and Image Resources. https://doi.org/10.5852/ejt.2026.1048.3247.14371